

# Measurement and comparison of silicon $p-i-n$ -photodiodes ac impedance at different voltages

© S. Özden, H. Bayhan<sup>†</sup>, A. Dönmez, M. Bayhan

University of Muğla, Faculty of Art and Science, Department of Physics,  
48000 Muğla, Turkey

(Получена 15 мая 2007 г. Принята к печати 12 сентября 2007 г.)

The dark alternating current (ac) parameters of commercially available silicon  $p-i-n$ -photodiodes are measured and compared at room temperature both in forward and reverse bias using the impedance spectroscopy technique. The ac behaviour of the photodiodes are found to be almost the same. For bias voltages in the range from  $-0.8$  to  $0.0$  V, the typical photodiode behaves like a pure capacitor. For higher voltages ( $V \geq 0.2$  V) the impedance spectra are nearly semicircle and typically distorted on the high frequency side. At  $0.2$  V the distortion apparently arises from one of the two interfaces. However, at high bias voltages the nature of the distortion is attributed to the variation of photodiode capacitance and resistance with measurement frequency.

PACS: 85.60.Dw, 73.40.Lq

## 1. Introduction

Silicon based  $p-i-n$ -photodiodes have tremendous potential in many applications such as in photo-interrupters, sensors, industrial electronics, control and drive circuits [1]. To design an efficient and reliable photodiode operation, both the static (dc) and the dynamic (ac) characteristics of a typical  $p-i-n$ -device need to be understood. In many applications the ac equivalent circuits are neglected and only the dc equivalent circuits are considered in the analysis of their response with the loads. Impedance spectroscopy (IS) has proved to be a powerful technique for studying the ac properties and hence the ac equivalent circuit modelling of organic, inorganic, ceramic and semiconductor materials and devices [2–4]. According to this technique, the complex impedance  $Z = Z' + jZ'' = (R + jX)$  of a device is measured directly in the frequency domain and a plot of the real (R) and imaginary (X) parts of the impedance on complex plane for varying frequency gives the impedance spectrum of the device. From this, the equivalent circuit parameters which are representative of the physical processes taking place in the device can be calculated.

In this study we investigate and compare the ac electrical response of typical silicon BPW 34 and BPW 41 (Vishay)  $p-i-n$ -photodiodes by varying the bias voltage from  $-0.8$  to  $+0.8$  V at room temperature. Frequency dependent data are obtained in the range from 100 Hz to 5 MHz.

## 2. Experimental

The dark ac impedance data of the photodiodes were measured using Hewlett Packard HP 4192A impedance analyser in the frequency ( $f$ ) range from 100 Hz to 10 MHz. The ac signal of amplitude 10 mV was selected to make accurate measurements and to ensure the operation conditions [5]. The photodiodes were mounted in the

sampler holder of the helium cryostat (Oxford) and all measurements were performed in vacuum. The room temperature impedance measurements were made at voltages between  $-0.8$  V and  $+0.8$  V in steps of 0.1 V.

## 3. Results and discussions

Nyquist plots of the typical BPW 34 and BPW 41 photodiodes at dc bias voltages varying from  $-0.8$  to  $+0.8$  V are shown in Fig. 1 (*a-d*). For bias voltages below 0.0 V the plots shown a straight line almost perpendicular to the R axis. As shown in Fig. 2, the Log–Log variation of the absolute impedance  $|Z| = \sqrt{R^2 + X^2}$  with frequency  $f$ , also yields a straight line over the whole frequency range in this low voltage region. All these indicate that both photodiodes behave like a pure capacitor for applied dc voltages in the range  $-0.8$  and  $0.0$  V. The impedance for a pure capacitor with capacitance  $C$ , is given as

$$Z = -j \frac{1}{\omega C} = -j(1/2\pi f C), \quad (1)$$

where  $\omega$  — angular frequency of the ac signal. Based on equation (1) and high frequency (1 MHz) impedance data measured at zero dc voltage, capacitances of 82 and 73 pF are inferred for BPW 34 and BPW 41, respectively. These are in well agreement with the values reported in the data sheets (Vishay–Telefunken) and measured by admittance spectroscopy under the same conditions.

When the bias voltage exceeds 0 V, although the impedance plots are very nearly semicircular in shape, they show some distortion at the high frequency side of the spectrum (Fig. 1, *a-d*). Since a typical silicon  $p-i-n$ -detector structure comprises an intrinsic layer sandwiched between two highly doped  $n$ - and  $p$ -type layers, the simplest and the typical equivalent circuit can be represented by two RC sub-circuits (parallel resistors  $R_{p1}$ ,  $R_{p2}$  and capacitors  $C_{01}$ ,  $C_{02}$ ) in series with a resistor  $R_s$ . However, the close inspection of the Bode plots given in Fig. 2, *a* and 2, *b*

<sup>†</sup> E-mail: hbayhan@mu.edu.tr

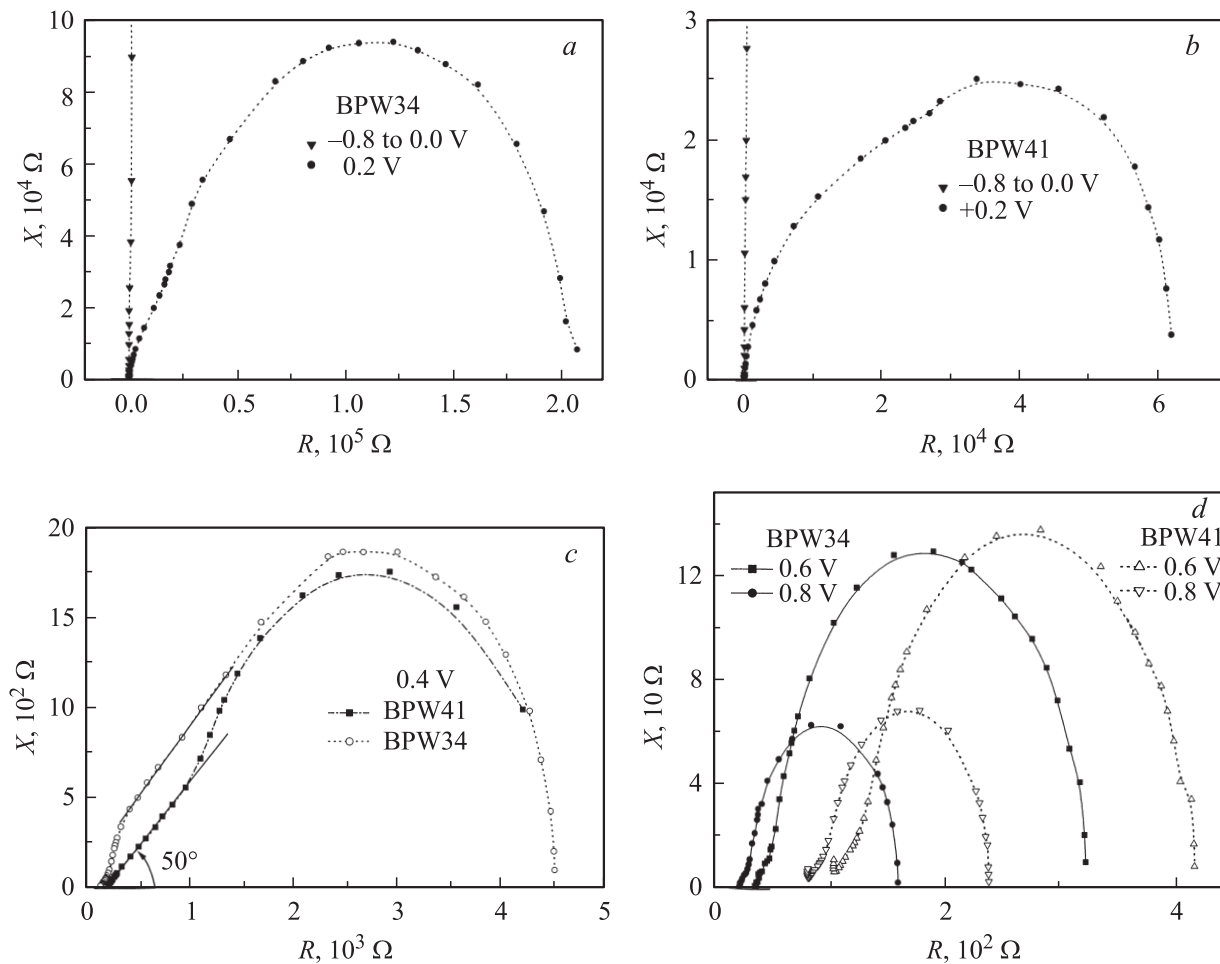


**Figure 1.**  $a-d$ . Nyquist plots of a typical BPW 34 and BPW 41 photodiodes at several bias voltages. The dotted lines are present to guide the eye.

clearly reveal that only the spectra measured at 0.2 V have multiple time constants. This suggests that both space charge regions namely,  $n/i$  and  $i/p$  interfaces could have important role for the ac response of the photodiodes.

At high bias voltages ( $0.4 \leq V \leq 0.80$  V), the phase angle  $\theta = \tan^{-1}(X/R)$  vs  $\text{Log } f$  plots of BPW 34 and BPW 41 yield a single peak at about 5.2 and 6 kHz as depicted in Fig. 2,  $a$  and  $2, b$ , respectively. Thus, in this voltage range the equivalent circuit can be designed as a single RC network in series with the resistor  $R_s$  for both photodiodes [2]. These suggest that either  $p/i$  or  $i/n$  interface could play a more relevant role for the ac conduction. Although we do not know the definite energy band structure and the doping profiles of different layers in the photodiodes, it is generally accepted that  $i$ -region in these devices is slightly  $n$ -type. If we assume that the  $n/i$ -junction is nearly ohmic, we can reasonably infer that the impedance characteristics are mainly determined by  $i/p$ -interface at forward bias voltages in between 0.4 and 0.8 V.

Fig. 1 also indicates that the semicircular nature of the impedance plots at high frequencies tend to a straight line

with a slope of around  $50^\circ$  for dc voltages higher than 0.2 V. This tendency decreases as one goes from 0.4 to 0.8 V. A possible physical origin for this deviation could be related to variation of device capacitance and resistance with the measurement frequency as similarly as reported for  $p-n$ -junction solar cells in the literature [5–8].

The electrical analogue circuit of a typical  $p-n$ -junction device can be described by a single RC network connected with a series resistance  $R_s$  which is proposed to be almost entirely created by the bulk layers and ohmic contacts. The RC network is composed by two types of capacitances and resistances which are all connected in parallel. They are [5,9]; diffusion and transition capacitances ( $C_d$  and  $C_T$ ) and resistances ( $R_d$  and  $R_T$ ), respectively.  $C_d$  and  $R_d$  are due to the gradient of the charge density inside the device and the bulk resistance of the space charge region, respectively.  $R_T$  — resistance due to recombination of free carriers in the space charge region and  $C_T$  — space charge layer capacitance.

The voltage dependent values for  $R_s$  and the equivalent parallel resistance combination ( $R_d \parallel R_T$ ) of the  $p-i-n$ -

devices are estimated from the low and high frequency intercepts of the semicircular variations on the  $x$ -axis of Figs. 1,  $a-d$ , respectively. The average value for the photodiode capacitance ( $C_T + C_d$ ) at different bias voltages are

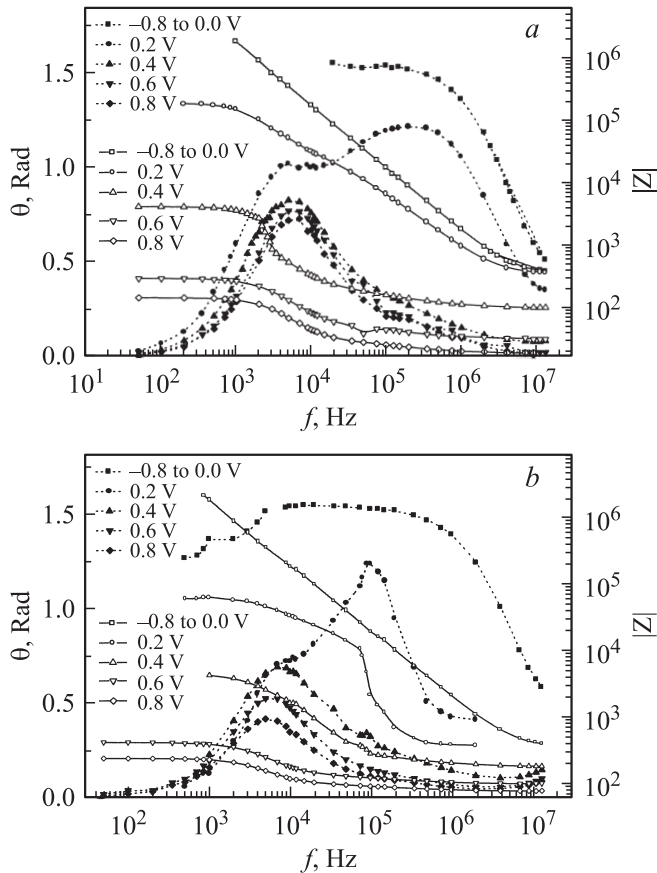


**Figure 2.** Bode plots of a typical (a) BPW 34 and (b) BPW 41 at different bias voltages. The open symbols correspond to the data for absolute magnitude of the impedance,  $|Z|$ , and the solid symbols correspond to the data for the phase angle,  $\theta$ . The dots and the lines are present to guide the eye.

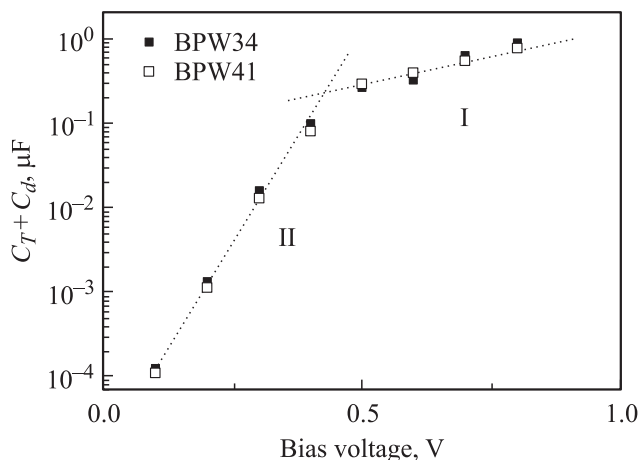


**Figure 3.** The variation of the photodiode capacitance with applied bias.

Variation of  $R_s$ ,  $C_T + C_d$  and  $R_d$  with different bias voltages

$V, V$	$R_s, \Omega$		$C_T + C_d, \mu F$		$R_d \parallel R_T (\Omega)$	
	BPW 34	BPW 41	BPW 34	BPW 41	BPW 34	BPW 41
0.2	340	500	$1.3 \cdot 10^{-3}$	$1.0 \cdot 10^{-3}$	207000	68500
0.3	—	—	$1.5 \cdot 10^{-2}$	$1.1 \cdot 10^{-2}$	—	—
0.4	100	210	$3.0 \cdot 10^{-2}$	$3.2 \cdot 10^{-2}$	4470	4150
0.5	—	—	$2.4 \cdot 10^{-1}$	$2.3 \cdot 10^{-1}$	—	—
0.6	36	100	$4.0 \cdot 10^{-1}$	$3.8 \cdot 10^{-1}$	286	300
0.7	—	—	$6.2 \cdot 10^{-1}$	$5.8 \cdot 10^{-1}$	—	—
0.8	20	80	$8.6 \cdot 10^{-1}$	$7.7 \cdot 10^{-1}$	138	147

estimated by using the value of  $R$  around maximum of  $X$  [5],

$$X_{\max} = \frac{1}{2\pi f (C_T + C_d)}. \quad (2)$$

All evaluated parameters are tabulated in Table 1. For further analysis of the origin of the photodiode capacitance at different bias voltages,  $C_T + C_d$  is plotted as a function of applied voltage in Fig. 3. It appears that the estimated capacitances of both photodiodes have almost the same variation with the applied bias voltage. The typical plot reveals the existence of two distinct linear regions. The capacitance shows a weak dependence on the applied voltage in region I which could possibly be due to the transition capacitance,  $C_T$ . The relatively strong linear dependence of  $\log(C_T + C_d)$  on the applied voltage in region II is attributed to the diffusion capacitance [8]. At high frequencies (i.e., for  $\omega\tau \gg 1$ , where  $\omega = 2\pi f$  and  $\tau$  — minority carrier lifetime) and under steady conditions,  $C_d$  is exponentially related to the applied voltage as [5]

$$C_d = \frac{\tau e}{nk} I_0 \exp(eV/nkT), \quad (3)$$

where  $e$  — electronic charge,  $k$  — Boltzmann constant,  $T$  — temperature,  $n$  — diode factor. The estimated value of  $n$  for both photodiodes is calculated from the slope of the linear variation in region I and found as about 1.59. This is almost equal to the average value of  $n$  determined from room temperature current-voltage data ( $n = 1.16$  and  $2.03$  for BPW 34 and for BPW 41, respectively).

## 4. Conclusion

The room temperature alternating current (ac) impedances of two different silicon  $p-i-n$ -photodiodes are studied and compared by varying the bias voltages from  $-0.8$  to  $+0.8$  V. This study shows that the ac parameters of both photodiodes are almost the same. For bias voltages smaller than  $0.2$  V the photodiodes behave like a pure capacitor. However, for higher forward bias ( $V \geq 0.2$  V) the impedance spectra are characterised by nearly semicircular shape apparently having some distortion in the high frequency region. The Bode plots have revealed that this distortion could be related to a second  $RC$ -network added to

one of the junction at 0.2 V. This suggest that both junctions namely,  $n/i$  and  $i/p$  interface could have important role for the ac response of the photodiodes.

However at higher bias voltages ( $0.4 \geq V \geq 0.8$  V), the predominance of a single time constant could possibly be correlated to the single sided junction operation of the device structure. The linearly shaped distortion observed in the high frequency region of the impedance plots is attributed to variation of the photodiode equivalent capacitance and the resistance with measurement frequency. The ac parameters of the photodiodes are estimated as a function of applied voltage which could be useful for electronic applications. The typical photodiode factor is estimated and found that it is almost equal to the average value calculated from current-voltage data of both photodiodes.

## References

- [1] Vishay Telefunken, *Data sheets of BPW34 and BPW41 photodiodes*. Available online at: <http://www.vishay.com/photodetectors> (2007).
- [2] J.R. Macdonald. *Impedance Spectroscopy* (Wiley, N. Y., 1987).
- [3] E. Barsoukov, J.R. Macdonald. *Impedance Spectroscopy: Theory, Experiment, and Applications*, 2nd edn (Wiley, Hoboken, N. J., 2005).
- [4] H. Bayhan, S. Ozden. *Semiconductors*, **41**, 353 (2007).
- [5] M.S. Suresh. *Sol. Energy Mater. Sol. Cells*, **43**, 21 (1996).
- [6] A. Kumar, M.S. Suresh, J. Nagaraju. *Sol. Energy Mater. Sol. Cells*, **60**, 155 (2000).
- [7] A.R. Kumar, M.S. Suresh. *Rev. Sci. Instrum.*, **72**, 3422 (2001).
- [8] A. Kumar, M.S. Suresh, J. Nagaraju. *Sol. Energy Mater. Sol. Cells*, **85**, 397 (2005).
- [9] H.S. Rauschenbach. *Solar Array Design Handbook* (Van Nostrand Reinhold, N. Y., 1980).

Редактор Л.В. Беляков